

# ENHANCING LLM FAITHFULNESS IN RATIONALE GENERATION VIA DUAL-REWARD PROBABILISTIC INFERENCE

000  
001  
002  
003  
004  
005 **Anonymous authors**  
006 Paper under double-blind review  
007  
008  
009  
010  
011  
012  
013  
014  
015  
016  
017  
018  
019  
020  
021  
022  
023  
024  
025  
026  
027  
028  
029  
030  
031  
032  
033  
034  
035  
036  
037  
038  
039  
040  
041  
042  
043  
044  
045  
046

## ABSTRACT

As large language models (LLMs) are increasingly applied to complex reasoning tasks, achieving both accurate task performance and faithful explanations becomes crucial. However, LLMs often generate unfaithful explanations, partly because they do not consistently adhere closely to the provided context. Existing approaches address this problem either rely on superficial calibration, such as decomposed Chain-of-Thought prompting, or require costly retraining to improve model faithfulness. In this work, we propose a probabilistic inference paradigm that provides fine-grained and lookahead rewards to ensure that LLM-generated rationales are logically coherent and comprehensive. These rewards are derived from a domain-specific proposal distribution, allowing for optimised sequential Monte Carlo approximations. Our evaluations across three different reasoning tasks show that this method, which allows for controllable generation during inference, improves both accuracy and faithfulness of LLMs while keeping computational costs similar to those of existing decoding techniques. This method offers a promising path towards making LLMs more reliable for reasoning tasks without sacrificing performance or efficiency.

## 1 INTRODUCTION

Large language models (LLMs) have achieved remarkable success across a wide range of challenging tasks, including Question Answering (QA) (Li et al., 2024b), reasoning (Yao et al., 2023; Yan et al., 2024) and providing feedback on essays or reviews (Liang et al., 2024; Li et al., 2023). However, the opaque nature of these models makes it difficult to generate faithful explanations for their decision-making processes. While LLMs can be prompted to generate self-explanations when making predictions (Kim et al., 2024; Madsen et al., 2024; Atanasova et al., 2023), ensuring the fidelity of these rationales remains challenging: both for improving interpretability and for enhancing reliability in safety-critical fields (Lyu et al., 2024).

Enhancing the faithfulness of LLM-generated rationales is a multifaceted challenge. To date, there is no universally accepted or formal definition of faithfulness (Lyu et al., 2024). In this paper, we focus on a specific category of unfaithfulness, where models fail to incorporate key contextual information into their generated rationales. It is motivated by faithfulness evaluation, where unfaithful models do not respond adequately to alterations in input (Lanham et al., 2023; Radhakrishnan et al., 2023). This example in Figure 1 highlights that the Llama3 tends to assign high probabilities to generic words, resulting in rationale that is less coherent with the given context. This limitation may contribute to potential unfaithfulness in the model’s outputs. In contrast, an expert model (logits in red), specifically trained on a scientific corpus, significantly increases the likelihood of domain-specific words that align more closely with the context. Moreover, the results presented in Table 1 show that the Llama3 exhibits a weak correlation between its generated assessments and the content of the provided in student’s reports, while the expert model shows significant improvements.

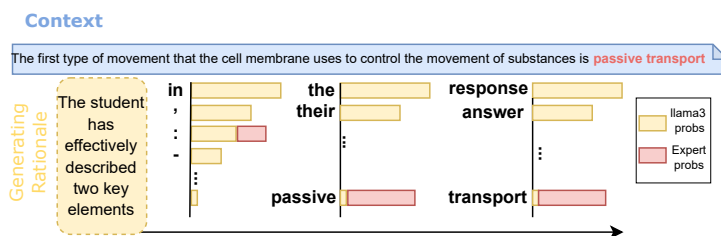


Figure 1: The decoding phrase in the untuned Llama3-8B-Instruct for assessing a student’s answer to a biology question. **Llama3 tends to generate overly generic words**, such as ‘*the*’ and ‘*response*’, while **ignoring domain-specific words in the context**. The expert model is more sensitive to and utilizes such domain-specific words in context, such as ‘*passive*’, ‘*transport*’.

The model’s tendency to rely heavily on its pretrained distributions can be attributed to its ignorance of context, often causing it to overlook subtle differences across various domains and contexts (Hu et al., 2023). Evidence from multiple studies suggests that LLMs often generate inaccurate labels when applied to out-of-distribution scenarios (Yuan et al., 2023). Lin et al. (2024) showed that instruction-tuned LLMs perform almost identically with base model in decoding across most token positions, suggesting that even advanced LLMs struggle with adapting to new domains and generating contextually sensitive responses.

To improve the model’s faithfulness by enhancing its sensitivity to context, we propose a **probabilistic inference paradigm** for generating faithful explanations. This approach incorporates *both local and anticipatory context coherence rewards* into a sequential Monte Carlo search. These rewards are inspired by the observation that LLMs struggle to generate domain-specific distributions due to their reliance on pretrained data. Specifically, we introduce a step-wise filtering proposal distribution that adjusts the generation distribution of original LLMs. This optimised distribution stands out by (i) being more sensitive to domain-specific nuances; and (ii) accounting for future rewards during the generation process. **Our contribution can be summarized as three-fold<sup>1</sup>:**

- We investigate the challenge of faithful rationale generation by highlighting the limitations of general LLMs in producing domain-specific responses. To the best of our knowledge, this is the first study to enhance faithfulness by explicitly encouraging the generation of domain-specific tokens.
- We propose two novel reward mechanisms, namely local and global rewards, tailored for the faithfulness problem. These are integrated into a probabilistic inference framework to achieve a trade-off between task accuracy and rationale faithfulness.
- Empirical results with the Llama 3 backbone model show an absolute accuracy improvement of 33% over the seven datasets, along with a 10% improvements in faithfulness evaluation, while maintaining a computational cost similar to beam search (1.3×).

## 2 RELATED WORK

**Constrained decoding.** Constrained generation can be accomplished by fine-tuning, such as RLHF (Ouyang et al., 2022) and DPO (Rafailov et al., 2023). Further inspired by the observations that alignment can be achieved by searching and planning in the large decoding space without costly training, many recent papers have proposed probabilistic inference. Many are focused on optimization, such as beam search (Meister et al., 2020), others focus on sampling from a constrained or modified distribution, including naive rejection sampling (Poesia et al., 2022), nucleus sampling (Holtzman et al., 2020) and also GFlowNet targeting at more diverse distribution (Bengio et al., 2021). Our solution is to adopt a domain-specific proposal distribution to adjust the original posterior.

<sup>1</sup>We will open-source our code on GitHub upon acceptance.

|        | <b>BLEU</b> | <b>Llama3</b> | <b>Expert</b> |
|--------|-------------|---------------|---------------|
| 2-gram | 0.085       | 0.683         |               |
| 3-gram | 0.081       | 0.544         |               |
| 4-gram | 0.076       | 0.436         |               |

Table 1: The **semantics overlap** between the student reports in the *biology* subject and the LLM-generated assessment rationales. Llama3-8B exhibits an overall lower overlap with the given context compared to a domain-specific expert model, implying a tendency towards unfaithfulness.

**Faithful rationale.** Although LLMs can provide plausibly sounding explanations for their answers, recent work argues that model generated natural language explanations are often unfaithful (Lanham et al., 2023; Atanasova et al., 2023). Faithfulness evaluation for rationale is to apply important perturbation to the original rationale and check the changes in the new output. Such perturbation includes counterfactual edit (Atanasova et al., 2023), biased feature (Turpin et al., 2023) and corrupted Chain-of-Thought (Lanham et al., 2023). To increase the faithfulness of LLM-generated response, many existing methods focus on the Chain-of-Thought and decompose the reasoning process into multiple sub-sentences (Radhakrishnan et al., 2023), then verify them using external tool, e.g., python interpreter (Lyu et al., 2023), counterfactual (Gat et al., 2023). The above methods alleviate the unfaithful issue either in a post-hoc manner or via costly training. We instead propose a inference-time method, which can improve both faithful and accurate for different reasoning tasks, also maintain a similar computation cost as beam search.

### 3 PROBABILISTIC INFERENCE FOR FAITHFUL RATIONALE GENERATION

We firstly introduce the faithfulness definition in our context, which serves as a foundation for our algorithm design (§3.2). Then, we frame the faithfulness-controllable generation problem as a form of posterior inference under constraints (§3.3). Finally, we elaborate on how our proposal distribution incorporates both local and global rewards to enhance faithfulness throughout the entire reasoning process (§3.4).

#### 3.1 PROBLEM DEFINITION

As our framework is grounded in a Monte Carlo search algorithm, we formalize the generation process as a search problem, represented as  $\langle S, \mathcal{V}, \pi, U \rangle$ . The state space  $S$  consists of multi-token sequences drawn from the vocabulary  $\mathcal{V}$ . The transition function  $\pi_t(x_{t+1} | x_t) \in \Delta^{|\mathcal{V}|}$  outputs a probability distribution over  $\mathcal{V}$ . The reward function  $U$  guides the search process. The objective is for the model to reach a terminal state defined by  $|eos|$  token, producing a sequence  $y = \langle v, v', \dots, |eos| \rangle$ . Special emphasis is placed on identifying a faithful rationale and achieving accurate answer prediction, guided by  $U$ .

#### 3.2 FAITHFUL RATIONALE GENERATION

Faithfulness is a crucial aspect of interpretability, and there are many different definitions and evaluation schema based on perturbation (Alvarez Melis & Jaakkola, 2018). Specially, we calculate the prediction difference before and after adding or removing important tokens from the input, i.e.,  $f(X) - f(X/I)$ , where  $X$  is input for the model  $f(\cdot)$  and  $I$  represents an important span within the input. This evaluation can be adapts to continuous changes, such as logits shifts and rationale changes (Siegel et al., 2024).

In our settings of LLM reasoning tasks, faithfulness applies to both the generated answers (such as classification labels in text classification tasks) and the rationales:

- The generated rationales should accurately reflect the true reasoning process, which can be assessed through perturbation.
- The label and rationale should be consistent with each other, i.e., the rationale should correctly reflect the predicted label.

In a broad sense, a faithful model would pay attention to the context provided (both the user query and the generated label) and make corresponding changes in their responses when facing with input context alterations. However, empirical observations (Lin et al., 2024) show that LLMs, even those instruction-tuned ones, tend to generate similar token distributions across most output positions. Inspired by the successes of injecting domain knowledge into LLMs reasoning (Ge et al., 2024), it could be promising to introduce domain-expert knowledge to make the model more sensitive and responsive to the given context.

---

141    3.3 PROBABILISTIC INFERENCE FOR RATIONALE GENERATION  
142

143 During LLM inference, the transition distribution (Markov chain)  $\pi$  is used to sample the next token given a  
144 prefix string according to the model’s pretrained distribution. Existing research shows that LLMs are inferior  
145 in generating accurate answers and faithful rationales for out-of-distribution inputs, sometimes performing  
146 even worse than pretrained smaller expert models (Yuan et al., 2023; Gekhman et al., 2024). Therefore, our  
147 goal here is to introduce reward from expert models to adjust the LLMs’ output distribution.  
148

149 **Background of Feynman-Kac model.** Feynman-Kac formulae (Del Moral & Del Moral, 2004) is de-  
150 signed to admit probabilistic sequential Monte Carlo approximation (Lew et al., 2023), which involves a  
151 tuple consisting of an initial state, a transition distribution, and a potential function  $(s_0, \pi_t, G_t)$ . In the con-  
152 text of generating tokens  $s_t$  using model  $f_\theta$ , The potential function  $G_t$  maps  $(s_t, s_{t+1})$  to a non-negative  
153 score, analogous to the reward function. The adjusted probability of  $f_\theta$  generates  $s_t$  is calculated as follows:  
154

155 
$$\mathbb{P}_t(s_t) = \frac{\mathbb{E}_\pi \left[ \prod_{i=1}^{t \wedge T} G_i(S_{i-1}, S_i, f_\theta) \cdot [S_t = s_t] \right]}{\mathbb{E}_\pi \left[ \prod_{i=1}^{t \wedge T} G_i(S_{i-1}, S_i, f_\theta) \right]}, \quad (1)$$
156

157 where  $[S_t = s_t]$  is an indicator function that is equal to 1 if the state at  $t$  is  $s_t$ , and 0 otherwise. The numerator  
158 inside the expectation represents the product of rewards and the probability of reaching state  $s_t$ , ensuring  
159 that paths leading to high rewards over time are given more weight. Generation continues until a terminal  
160 token or the maximum length of the sequence  $T$ , i.e.,  $t \wedge T = \min(t, T)$ .  
161

162 **Probabilistic inference for faithful rationale generation.** We develop our faithfulness-seeking model  
163 based on the Feynman-Kac framework primarily for its *computation efficiency* and *lookahead rewards*. Un-  
164 like existing *explicit* MCTS requiring expensive rollouts or simulations to evaluate potential actions (Xie  
165 et al., 2024; Zhang et al., 2024a; openai, 2024), it computes expected rewards in a more integrated and  
166 efficient way, streamlining the inference process. The incorporated lookahead  $G(s_{t-1}, s_t)$  is achieved on  
167 cumulative rewards across multiple steps , rather than overly prioritize short-term gains or rely on heuristics,  
168 e.g., the normalized average (Wang et al., 2024) that do not model future states effectively.  
169

170 In our settings, the generated sequence for reasoning tasks consists of an answer and an explanation <sup>2</sup>.  
171 The design of the faithfulness-related potential function takes into account (i) the accuracy of the predicted  
172 answer and (ii) the faithful rationale that explains the prediction. Since the answer is generated first without  
173 considering the subsequent context, whereas a faithful rationale requires coherence with the surrounding  
174 context, we introduce a local expert and a lookahead expert to address these two aspects. The generation  
175 framework is outlined in Algorithm 1: Dual-Reward Probabilistic Inference, with functions LOCALMASK  
176 and GLOBALREWARD.  
177

178 At each timestep during model inference, both the local and global experts calculate a weight, denoted as  $\alpha_t$ ,  
179 for the generated token  $x_t$ . Similar to beam search, we generate  $K$  branches and select the generated trajec-  
180 tory with the highest sequence-level weight. For the local reward, we adjust the token’s probability to favor  
181 predictions that align with the local expert’s output  $c_0$ . For the global reward, which encourages rational  
182 generation, we use the global expert model  $g$  to score the current token  $x_t$  based on future predictions.  
183

184    3.4 SEARCH WITH DUAL-REWARD  
185

186 **Local mask.** One heuristic and lightweight approach to constrained generation from LLMs is to use mask-  
187 ing or logit bias to reweigh the probabilities of sampled tokens, i.e.,  $\pi_t$ . Many existing methods (Liu et al.,  
188 2024a; Zhao et al., 2024) leverage generation logits from smaller models to calibrate the logits from larger  
189

190 <sup>2</sup>To prevent scenarios where an overly long rationale causes the answer to exceed the output length limit, we prioritize  
191 generating the answer first. Our framework can be extended to tasks where the answer space is infinite (Appendix C.1).  
192



Genre Natural Language Inference (MNLI) (Williams et al., 2018) datasets; and *TruthfulQA* dataset (Lin et al., 2022). In each of these tasks, LLMs are required to generate both class labels and rationales justifying their classification decisions. For student answer assessment, the labels represent valid score ranges, 0-5; For NLI, the labels are ‘*entailment*’, ‘*contradiction*’, or ‘*neutral*’. For *TruthfulQA*, we use a subset of the dataset converted into a multiple-choice format.

**Backbone models and expert models.** Our study employs two widely used instruction-tuned LLMs as our backbone models: Llama-3-8B-Instruct (Dubey et al., 2024) and Mistral-7B-Instruct-v0.3 (Jiang et al., 2023)<sup>4</sup>. For each dataset, we incorporate one expert model for local reward and another expert model to offer global reward. The details are shown in Appendix A. Note that all the expert models are only fine-tuned on the validation subset. It is worth noting that our framework can integrate with various expert models, even when their tokenization spaces differ from the backbone models.

#### 4.1 MAIN RESULTS OF TASK PERFORMANCE

**Our method significantly outperforms the backbone model, achieving a substantial performance improvement.** The experimental results summarized in Table 2 highlight the efficacy of our decoding method, which combines both local and global rewards, compared to the baseline Llama3 across various NLP tasks. Due to limited computational resources, our experiments are evaluated on 100 randomly sampled instances from each dataset, with the model utilizing 8-bit quantization. Results show the consistent enhancement in task performance achieved by our method without any further tuning of the backbone model on task-specific datasets. Specially, our reward-based decoding strategy achieves an average 40% improvement in accuracy on *Student Answer Scoring*, a 20% improvement on *NLI*, and a 26% increment on *TruthfulQA*.

#### 4.2 RATIONALE FAITHFULNESS EVALUATION

**Perturbation.** Following existing approaches for counterfactual generation in faithfulness evaluation, we modify key parts  $w$  of the inputs  $I$  and observe the resultant variations in the generated rationales. For *student answer assessment*, we remove the clause (sub-sentence) from the student answer that is most semantically related to the original rationale  $R_o$ . In the case of *NLI* and *TruthfulQA*, where the sentences in the provided context are typically very short (often a single sentence), we introduce perturbations through word insertion, as inspired by Atanasova et al. (2023). Specifically, we apply POS tagging to the sentence in the context to identify verbs and adjectives which are likely to have a greater impact and replace them with alternative words. We then feed the perturbed input to the model for new rationale  $R_n$ . The algorithm for generating counterfactual rationales is detailed in the Appendix A.

**Evaluation Metrics.** For the sub-sentence removal perturbation, we calculate the semantic relatedness between the removed text span  $w$  and the original rationale, denoted as  $S_{wo} = \text{Sim}(w, R_o)$ , and between the removed span and the new rationale, denoted as  $S_{wn} = \text{Sim}(w, R_n)$ . A faithful model is expected to produce a significant **semantic variation**, i.e.,  $\Delta(S_{wo} - S_{wn})$ , as the removed sub-sentence should be closely related to the original rationale but less similar to the new rationale. For the word *insertion* perturbation, we calculate the percentage of new rationales that include the newly inserted word, denoted as **word inclusion**. Both large semantic variation and word inclusion indicates a better faithfulness.

<sup>4</sup>The results of Mistral is presented in Table 8 in Appendix.

| Datasets                          | Llama3 | Ours       |
|-----------------------------------|--------|------------|
| <i>Student Answer Assessment</i>  |        |            |
| ASAP-Q1                           | 28%    | <b>57%</b> |
| ASAP-Q2                           | 28%    | <b>68%</b> |
| ASAP-Q3                           | 45%    | <b>90%</b> |
| ASAP-Q4                           | 38%    | <b>84%</b> |
| <i>Natural Language Inference</i> |        |            |
| SNLI                              | 49%    | <b>69%</b> |
| MNLI                              | 57%    | <b>77%</b> |
| <i>Question-Answering</i>         |        |            |
| TruthfulQA                        | 47%    | <b>73%</b> |

Table 2: Task performances (Accuracy) across three tasks between Llama3 and our proposed method.

as the removed sub-sentence should be closely related to the original rationale but less similar to the new rationale. For the word *insertion* perturbation, we calculate the percentage of new rationales that include the newly inserted word, denoted as **word inclusion**. Both large semantic variation and word inclusion indicates a better faithfulness.

282  
283

## 4.2.1 RESULTS OF FAITHFULNESS EVALUATION

284  
285  
286  
287  
288  
289  
290  
291

**Results on student answer assessment.** Table 3 compares the semantic variations  $\Delta(S_{wo} - S_{wn})$  measured in ROUGE scores (R-1, R-2 and R-L). We expect that we can observe in Table 3 that the variation in ROUGE scores across different subsets demonstrates the effectiveness of our method in generating more faithful rationales compared to the baseline model. Our method shows significantly enlarged ROUGE-L score differences for all the subsets except for Q2, indicating a substantial lexical difference with the removed content after applying counterfactual modifications. For Q4, the notable increase in all ROUGE metrics highlights a pronounced enhancement in the model’s ability to retain relevant information despite the removal of critical sub-sentences.

292

| Method | ASAP-Q1      |              |              | ASAP-Q2      |              |              | ASAP-Q3      |              |              | ASAP-Q4      |              |              |
|--------|--------------|--------------|--------------|--------------|--------------|--------------|--------------|--------------|--------------|--------------|--------------|--------------|
|        | R-1          | R-2          | R-L          |
| Llama3 | 0.037        | <b>0.043</b> | 0.034        | 0.052        | <b>0.050</b> | <b>0.052</b> | 0.042        | 0.031        | 0.043        | 0.006        | 0.018        | 0.001        |
| Ours   | <b>0.064</b> | 0.035        | <b>0.052</b> | <b>0.056</b> | 0.029        | 0.050        | <b>0.064</b> | <b>0.051</b> | <b>0.058</b> | <b>0.105</b> | <b>0.085</b> | <b>0.102</b> |

296  
297

Table 3: The faithfulness on student answer scoring dataset, i.e., sentence-level semantic variations measured in ROUGE scores.

298  
299  
300  
301  
302  
303  
304

**Results for NLI and QA.** The word inclusion metric in Table 4 enriches our analysis by quantifying the extent to which perturbed input tokens are reflected in the generated rationales. For the *SNLI*, word inclusion increases by 4%, and for the *MNLI* dataset, it raises by 9%. These increases suggest that our model not only modifies its responses but does so in a way that better captures the new input elements. For *TruthfulQA*, our improvements are significantly more pronounced, with a 16% enhancement in performance. These higher inclusion rates highlight the model’s capacity to maintain high fidelity to the input semantic changes.

305  
306

## 5 MODEL ABLATION AND CASE STUDY

307

| Datasets<br>(Backbone)           | Expert Model |            | Our + Expert Model |             |              |
|----------------------------------|--------------|------------|--------------------|-------------|--------------|
|                                  | CLS          | Expert     | Ours+CLS           | Ours+Expert | Our(Full)    |
| <i>Student Answer Assessment</i> |              |            |                    |             |              |
| Q1 (28%)                         | 85%          | <b>76%</b> | 55%                | 45%         | 57% ↑        |
| Q2 (28%)                         | 72%          | 48%        | 51%                | 52%         | <b>68% ↑</b> |
| Q3 (45%)                         | 91%          | 71%        | 64%                | 79%         | <b>90% ↑</b> |
| Q4 (38%)                         | 88%          | 67%        | 66%                | 71%         | <b>84% ↑</b> |
| <i>NLI</i>                       |              |            |                    |             |              |
| SNLI (49%)                       | 86%          | <b>76%</b> | 54%                | 54%         | 69% ↑        |
| MNLI (57%)                       | 88%          | 76%        | 41%                | 61%         | <b>77% ↑</b> |
| <i>TruthfulQA</i>                |              |            |                    |             |              |
| TruthQA (47%)                    | 100%         | 70%        | 30%                | 46%         | <b>73% ↑</b> |

318  
319

Table 5: Ablation performance across three datasets in accuracy. ↑ denotes better than backbone.

320  
321  
322

## 5.1 EFFECTS OF LOCAL AND GLOBAL REWARD

We show the results of ablating the local reward, i.e., classifier (CLS) and global reward, i.e., Expert for task performance and faithfulness in Table 5 and Table 6.

323  
324  
325  
326  
327  
328

**Local reward contributes to task performance.** We observe significant performance improvements by introducing the local reward over *student answer assessment* and *SNLI*. The increment is due to the expertise of local reward in classification. Notably, when incorporating the CLS, our method does not necessarily perform as well as the classifier alone. This is partly because we could only penalize the words in label space but not all synonyms to the label word. For example, in *MNLI*, the model insists on ‘*polarization*’ even we lower the probability of ‘*contradictory*’.

| Dataset | Llama3 | Ours       |
|---------|--------|------------|
| SNLI    | 11%    | <b>15%</b> |
| MNLI    | 9%     | <b>18%</b> |

Table 4: Faithfulness on *NLI* and *TruthfulQA* tasks on word inclusive.

| Dataset<br>(Backbone)                                   | Expert<br>model | Our+Expert   |                |
|---|-----------------|--------------|----------------|
|   |                 | Our+Expert   | Our(full)      |
| <i>Student Answer Assessment</i> (semantic variation ↑) |                 |              |                |
| Q1 (0.034)  | <b>0.094</b>    | 0.032        | 0.052 ↑        |
| Q2 (0.051)  | <b>0.114</b>    | 0.048        | 0.050          |
| Q3 (0.042)  | <b>0.061</b>    | 0.037        | 0.058 ↑        |
| Q4 (0.001)  | 0.085           | 0.053 ↑      | <b>0.102</b> ↑ |
| <i>NLI</i> (Word inclusive ↑)                           |                 |              |                |
| SNLI (11%)  | 13%             | <b>22% ↑</b> | 15% ↑          |
| MNLI (9%)   | 9%              | <b>19% ↑</b> | <b>19% ↑</b>   |
| <i>QA</i> (Word inclusive ↑)                            |                 |              |                |
| TruthfulQA(2%)  | <b>24%</b>      | 19% ↑        | 18% ↑          |

Table 6: Ablation performance across three datasets in faithfulness. ↑ denotes better than backbone.

**Global reward contributes to both task performance and faithfulness.** From Table 5, with the incorporation of global expert, we achieve a better task performance than backbone on all datasets except *TruthfulQA*. Some improvements are even higher than CLS, especially on the *Q2-Q4, MNLI*. It can be explained that the task performance can also benefit from domain knowledge, which is consistent with the observations in Ge et al. (2024). From Table 6, Expert enhances the model faithfulness across the three benchmarks, although slightly lower on Q1-Q3, its improvements on Q4 is much more significant, from 0.001 to 0.053.

**Local reward fails to give look-ahead control by comparing with logitfusion (Liu et al., 2024a).** It is expected that our proposed local constraint is mainly for providing accurate label information, rather than rationale generation. To highlight the advantages of our global reward, we compare with a decoding method with local constraint (Liu et al., 2024a), which fuses the generated token probability from the expert and the backbone models at each timestep via interpolation. As shown in Table 7, rationales generated from logits fusion baseline are among 55% less faithful on average compared with ours (displayed in Table 3) <sup>5</sup>, their task performance is even lower than some of the backbone results. Moreover, logit fusion does not support fusion between models with different tokenization. The theoretical advantage between logit fusion and our look-ahead reward is that our method *considers future tokens' plausibility when scoring the currently generated token*. The potential function  $U^g$  at timestep  $t$  considers the generated sequence until  $l$  steps ahead.

| Datasets | Acc        | Faithfulness |
|----------|------------|--------------|
| Q1       | 34% (-40%) | 0.028 (-46%) |
| Q2       | 22% (-68%) | 0.037 (-26%) |
| Q3       | 40% (-56%) | 0.019 (-67%) |
| Q4       | 29% (-65%) | 0.019 (-81%) |
| Avg      | 31% (-57%) | 0.026 (-55%) |

Table 7: Logit fusion results on both task performance and faithfulness for student essay assessment. The relative changes compared with ours are in the bracket.

**Local and global rewards jointly achieves the overall best task performance and faithfulness.** Interestingly, our full model outperforms the inclusive of either CLS or Expert alone, achieving the best task performance across all seven datasets and demonstrating greater faithfulness than Our+GExpert in five of them. This joint effect can be inspired by pruned Monte Carlo search, where undesirable branches are eliminated. Similarly, our local constraint serves the same purpose by removing trajectories that lead to undesirable label words. More strictly, combined with the stochastic nature of the decoding process, we give a proof that branch pruning can lead to different search trajectories in Appendix D. This explains why our full model achieves overall better performance than one that solely incorporates the Expert model.

## 5.2 DOMAIN-SPECIFIC WORD DISTRIBUTION

We utilize TF-IDF to select domain-specific words (after removing the stopwords) from the student responses in the *student answer assessment* dataset. The selected words and their associated TF-IDF scores are depicted in the blue curve (context) in Figure 2. Since the TF-IDF score reflects the importance of these contextual words, we calculate the TF-IDF scores for the same words within the rationales generated by the backbone model (in orange) and our-full model (in green). This allows us to verify whether the generated rationales align well with the important spans in the context. It is clear that the green curve is mostly above the orange curve,

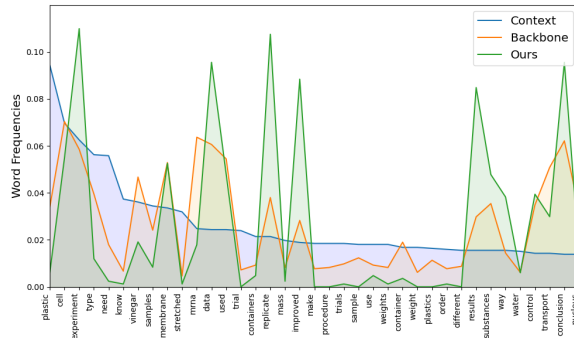


Figure 2: Distribution of domain-specific word.

<sup>5</sup>Note that more than 50% of the samples failed to generate responses due to the fused logit being impractical for the backbone model.

376 showing that our method can respond more actively to those domain-specific words, such as “*experiment*”,  
 377 “*data*”, “*replicate*”, “*substances*”, and “*nuclear*”.  
 378

379 **5.3 CASE STUDIES**  
 380

381 To highlight the differences between the rationales from the backbone model and ours, we randomly select  
 382 two examples from *Student Answer Assessment* and *Natural Language Inference* datasets, as shown in case  
 383 study 5.3. For the student answer assessment task, there are three key elements (highlighted in colour)  
 384 mentioned in the context, such as *how much vinegar*, *what size surface*. The student response also mentioned  
 385 these key concepts. In the rationale generated by the backbone, its feedback is not aligned well with the key  
 386 concepts, like ‘*fails to specify the vinegar type, drying method*’. Instead, our generated rationale closely  
 387 related to the two elements (spans are highlighted in colours).  
 388

389 For the *NLI* dataset, we present a perturbation example where the word *frugally* is inserted at the beginning  
 390 of the context. Our method-generated rationale could capture this word sensitively and be reflected in the  
 391 rationale content. While the backbone model acts less robust, it completely ignores this new insertion and  
 392 incorrectly predicts the label.  
 393

**Case studies**

**Student Answer Assessment**

395 **Key Answer Elements:** (i) how much vinegar was used in each container. (ii) what size/surface area of  
 396 materials should be used. (iii) what drying method to use. . .

397 **Student Response:** “Some example of things you would need to no is *how much vinegar is being poured in*  
 398 *each of the separate containers*. Another thing is the volume of each substance because the *surface area will*  
 399 *effect* how much is eroded off. Another thing where you let the samples sit for 30 minutes because there  
 400 might be *difference in temperature effecting how much it dries*.”

- 401 \* **Backbone:** Score: 1 point; The student has provided a valid concern about the need for specific information  
 402 to replicate the experiment, but only mentions three key details that would be necessary to know, *and fails*  
 403 *to specify the type of vinegar used, drying method*, or other important details.
- 404 \* **Ours:** 2 points; The student’s response describes two additional pieces of information that would be needed  
 405 to accurately replicate the experiment, *the amount of vinegar used* and *the size/surface area of the materials*.

**Natural Language Inference**

406 **Perturbed Premise:** *frugally* Requires free registration.

407 **Hypothesis:** Does not require free registration.

- 408 \* **Backbone:** Entailment; Requires free registration is a necessary condition for only if Requires free regis-  
 409 tration.
- 410 \* **Ours: Contradiction:** The premise states that the website [*frugally*] requires free registration, which implies  
 411 that a user must provide some information or sign.

414 **6 CONCLUSION**  
 415

416 In this paper, we address the critical challenge of enhancing both accuracy and faithfulness in large language  
 417 models. Specially, we introduce a probabilistic inference paradigm that incorporates fine-grained and look-  
 418 ahead rewards to search desirable trajectories. Compared to existing inference-time solutions, our method  
 419 distinguishes itself through a domain-specific proposal distribution that increases the model’s responsiveness  
 420 to key words in the context. We verify the effectiveness of our approach across three diverse datasets, eval-  
 421 uating both task performance and faithfulness metrics. Furthermore, our model ablation study demonstrates  
 422 the superiority of integrating both local and global rewards.

423 REFERENCES  
424

- 425 David Alvarez Melis and Tommi Jaakkola. Towards robust interpretability with self-explaining neural net-  
426 works. *Advances in neural information processing systems*, 31, 2018.
- 427 Pepa Atanasova, Oana-Maria Camburu, Christina Lioma, Thomas Lukasiewicz, Jakob Grue Simonsen,  
428 and Isabelle Augenstein. Faithfulness tests for natural language explanations. In Anna Rogers, Jordan  
429 Boyd-Graber, and Naoaki Okazaki (eds.), *Proceedings of the 61st Annual Meeting of the Association  
430 for Computational Linguistics (Volume 2: Short Papers)*, pp. 283–294, Toronto, Canada, July  
431 2023. Association for Computational Linguistics. doi: 10.18653/v1/2023.acl-short.25. URL <https://aclanthology.org/2023.acl-short.25>.
- 433 Emmanuel Bengio, Moksh Jain, Maksym Korablyov, Doina Precup, and Yoshua Bengio. Flow  
434 network based generative models for non-iterative diverse candidate generation. In M. Ranzato,  
435 A. Beygelzimer, Y. Dauphin, P.S. Liang, and J. Wortman Vaughan (eds.), *Advances in Neural  
436 Information Processing Systems*, volume 34, pp. 27381–27394. Curran Associates, Inc.,  
437 2021. URL [https://proceedings.neurips.cc/paper\\_files/paper/2021/file/e614f646836aaed9f89ce58e837e2310-Paper.pdf](https://proceedings.neurips.cc/paper_files/paper/2021/file/e614f646836aaed9f89ce58e837e2310-Paper.pdf).
- 439 Samuel R. Bowman, Gabor Angeli, Christopher Potts, and Christopher D. Manning. A large annotated  
440 corpus for learning natural language inference. In Lluís Màrquez, Chris Callison-Burch, and Jian Su  
441 (eds.), *Proceedings of the 2015 Conference on Empirical Methods in Natural Language Processing*, pp.  
442 632–642, Lisbon, Portugal, September 2015. Association for Computational Linguistics. doi: 10.18653/  
443 v1/D15-1075. URL <https://aclanthology.org/D15-1075>.
- 445 Oana-Maria Camburu, Tim Rocktäschel, Thomas Lukasiewicz, and Phil Blunsom. e-snli: Natural language  
446 inference with natural language explanations. In S. Bengio, H. Wallach, H. Larochelle, K. Grauman,  
447 N. Cesa-Bianchi, and R. Garnett (eds.), *Advances in Neural Information Processing Systems*, volume 31.  
448 Curran Associates, Inc., 2018. URL [https://proceedings.neurips.cc/paper\\_files/paper/2018/file/4c7a167bb329bd92580a99ce422d6fa6-Paper.pdf](https://proceedings.neurips.cc/paper_files/paper/2018/file/4c7a167bb329bd92580a99ce422d6fa6-Paper.pdf).
- 450 Pierre Del Moral and Pierre Del Moral. *Feynman-kac formulae*. Springer, 2004.
- 452 Abhimanyu Dubey, Abhinav Jauhri, et al. The llama 3 herd of models, 2024. URL <https://arxiv.org/abs/2407.21783>.
- 454 Yair Gat, Nitay Calderon, Amir Feder, Alexander Chapanin, Amit Sharma, and Roi Reichart. Faithful expla-  
455 nations of black-box nlp models using llm-generated counterfactuals. *arXiv preprint arXiv:2310.00603*,  
456 2023.
- 458 Yingqiang Ge, Wenyue Hua, Kai Mei, Juntao Tan, Shuyuan Xu, Zelong Li, Yongfeng Zhang, et al. Openagi:  
459 When llm meets domain experts. *Advances in Neural Information Processing Systems*, 36, 2024.
- 460 Zorik Gekhman, Gal Yona, Roee Aharoni, Matan Eyal, Amir Feder, Roi Reichart, and Jonathan Herzig.  
461 Does fine-tuning llms on new knowledge encourage hallucinations? *CoRR*, abs/2405.05904, 2024. doi:  
462 10.48550/ARXIV.2405.05904. URL <https://doi.org/10.48550/arXiv.2405.05904>.
- 464 Pengcheng He, Jianfeng Gao, and Weizhu Chen. Debertav3: Improving deberta using electra-style pre-  
465 training with gradient-disentangled embedding sharing, 2023. URL <https://arxiv.org/abs/2111.09543>.
- 467 Ari Holtzman, Jan Buys, Li Du, Maxwell Forbes, and Yejin Choi. The curious case of neural text degenera-  
468 tion. In *International Conference on Learning Representations*, 2020. URL <https://openreview.net/forum?id=rygGQyrFvH>.

- 470 Edward J Hu, Moksh Jain, Eric Elmoznino, Younesse Kaddar, Guillaume Lajoie, Yoshua Bengio, and Nikolay  
 471 Malkin. Amortizing intractable inference in large language models. *arXiv preprint arXiv:2310.04363*,  
 472 2023.
- 473 Albert Q. Jiang, Alexandre Sablayrolles, Arthur Mensch, Chris Bamford, Devendra Singh Chaplot, Diego  
 474 de las Casas, Florian Bressand, Gianna Lengyel, Guillaume Lample, Lucile Saulnier, Lélio Renard  
 475 Lavaud, Marie-Anne Lachaux, Pierre Stock, Teven Le Scao, Thibaut Lavril, Thomas Wang, Timothée  
 476 Lacroix, and William El Sayed. Mistral 7b, 2023. URL <https://arxiv.org/abs/2310.06825>.
- 477 Kyungha Kim, Sangyun Lee, Kung-Hsiang Huang, Hou Pong Chan, Manling Li, and Heng Ji. Can llms pro-  
 478 duce faithful explanations for fact-checking? towards faithful explainable fact-checking via multi-agent  
 479 debate. *ArXiv*, abs/2402.07401, 2024. URL <https://api.semanticscholar.org/CorpusID:267627437>.
- 480 Tamera Lanham, Anna Chen, Ansh Radhakrishnan, Benoit Steiner, Carson E. Denison, Danny Hernandez,  
 481 Dustin Li, Esin Durmus, Evan Hubinger, John Kernion, Kamil.e Lukovsiute, Karina Nguyen, Newton  
 482 Cheng, Nicholas Joseph, Nicholas Schiefer, Oliver Rausch, Robin Larson, Sam McCandlish, Sandi-  
 483 pan Kundu, Saurav Kadavath, Shannon Yang, Tom Henighan, Timothy D. Maxwell, Timothy Telleen-  
 484 Lawton, Tristan Hume, Zac Hatfield-Dodds, Jared Kaplan, Janina Brauner, Sam Bowman, and Ethan  
 485 Perez. Measuring faithfulness in chain-of-thought reasoning. *ArXiv*, abs/2307.13702, 2023. URL  
 486 <https://api.semanticscholar.org/CorpusID:259953372>.
- 487 Alexander K. Lew, Tan Zhi-Xuan, Gabriel Grand, and Vikash K. Mansinghka. Sequential monte carlo  
 488 steering of large language models using probabilistic programs. *ArXiv*, abs/2306.03081, 2023. URL  
 489 <https://api.semanticscholar.org/CorpusID:259075836>.
- 490 Mike Lewis, Yinhan Liu, Naman Goyal, Marjan Ghazvininejad, Abdelrahman Mohamed, Omer Levy,  
 491 Veselin Stoyanov, and Luke Zettlemoyer. BART: Denoising sequence-to-sequence pre-training for natu-  
 492 ral language generation, translation, and comprehension. In Dan Jurafsky, Joyce Chai, Natalie Schluter,  
 493 and Joel Tetreault (eds.), *Proceedings of the 58th Annual Meeting of the Association for Compu-  
 494 tational Linguistics*, pp. 7871–7880, Online, July 2020. Association for Computational Linguistics. doi:  
 495 10.18653/v1/2020.acl-main.703. URL <https://aclanthology.org/2020.acl-main.703>.
- 496 Jiazheng Li, Lin Gui, Yuxiang Zhou, David West, Cesare Aloisi, and Yulan He. Distilling ChatGPT  
 497 for explainable automated student answer assessment. In *Findings of the Association for Compu-  
 498 tational Linguistics: EMNLP 2023*. Association for Computational Linguistics, 2023. URL <https://aclanthology.org/2023.findings-emnlp.399>.
- 499 Jiazheng Li, Hainiu Xu, Zhaoyue Sun, Yuxiang Zhou, David West, Cesare Aloisi, and Yulan He. Calibrating  
 500 llms with preference optimization on thought trees for generating rationale in science question scoring,  
 501 2024a. URL <https://arxiv.org/abs/2406.19949>.
- 502 Zhenyu Li, Sunqi Fan, Yu Gu, Xiuxing Li, Zhichao Duan, Bowen Dong, Ning Liu, and Jianyong Wang.  
 503 Flexkbqa: A flexible lilm-powered framework for few-shot knowledge base question answering. In *Pro-  
 504 ceedings of the AAAI Conference on Artificial Intelligence*, volume 38, pp. 18608–18616, 2024b.
- 505 Weixin Liang, Yuhui Zhang, Hancheng Cao, Binglu Wang, Daisy Yi Ding, Xinyu Yang, Kailas Vodrahalli,  
 506 Siyu He, Daniel Scott Smith, Yian Yin, et al. Can large language models provide useful feedback on  
 507 research papers? a large-scale empirical analysis. *NEJM AI*, 1(8):A10a2400196, 2024.
- 508 Bill Yuchen Lin, Abhilasha Ravichander, Ximing Lu, Nouha Dziri, Melanie Sclar, Khyathi Chandu, Chandra  
 509 Bhagavatula, and Yejin Choi. The unlocking spell on base LLMs: Rethinking alignment via in-context  
 510 learning. In *The Twelfth International Conference on Learning Representations*, 2024. URL <https://openreview.net/forum?id=wxJ0eXwwda>.

- 517 Stephanie Lin, Jacob Hilton, and Owain Evans. TruthfulQA: Measuring how models mimic human falsehoods.  
 518 In Smaranda Muresan, Preslav Nakov, and Aline Villavicencio (eds.), *Proceedings of the 60th*  
 519 *Annual Meeting of the Association for Computational Linguistics (Volume 1: Long Papers)*, pp. 3214–  
 520 3252, Dublin, Ireland, May 2022. Association for Computational Linguistics. doi: 10.18653/v1/2022.  
 521 acl-long.229. URL <https://aclanthology.org/2022.acl-long.229>.
- 522 Alisa Liu, Xiaochuang Han, Yizhong Wang, Yulia Tsvetkov, Yejin Choi, and Noah A. Smith. Tuning  
 523 language models by proxy. In *First Conference on Language Modeling*, 2024a. URL <https://openreview.net/forum?id=dribhnhm1i>.
- 524 Jiacheng Liu, Andrew Cohen, Ramakanth Pasunuru, Yejin Choi, Hannaneh Hajishirzi, and Asli Celikyilmaz.  
 525 Don’t throw away your value model! generating more preferable text with value-guided monte-carlo tree  
 526 search decoding. In *First Conference on Language Modeling*, 2024b. URL <https://openreview.net/forum?id=kh9Zt2Ldmn>.
- 527 Qing Lyu, Shreya Havaldar, Adam Stein, Li Zhang, Delip Rao, Eric Wong, Marianna Apidianaki, and Chris  
 528 Callison-Burch. Faithful chain-of-thought reasoning. In Jong C. Park, Yuki Arase, Baotian Hu, Wei Lu,  
 529 Derry Wijaya, Ayu Purwarianti, and Adila Alfa Krisnadhi (eds.), *Proceedings of the 13th International*  
 530 *Joint Conference on Natural Language Processing and the 3rd Conference of the Asia-Pacific Chapter of*  
 531 *the Association for Computational Linguistics (Volume 1: Long Papers)*, pp. 305–329, Nusa Dua, Bali,  
 532 November 2023. Association for Computational Linguistics. doi: 10.18653/v1/2023.ijcnlp-main.20. URL  
 533 <https://aclanthology.org/2023.ijcnlp-main.20>.
- 534 Qing Lyu, Marianna Apidianaki, and Chris Callison-Burch. Towards faithful model explanation in nlp: A  
 535 survey. *Computational Linguistics*, pp. 1–67, 2024.
- 536 Andreas Madsen, Sarath Chandar, and Siva Reddy. Are self-explanations from large language models  
 537 faithful? In Lun-Wei Ku, Andre Martins, and Vivek Srikumar (eds.), *Findings of the Association*  
 538 *for Computational Linguistics ACL 2024*, pp. 295–337, Bangkok, Thailand and virtual meeting, Au-  
 539 gust 2024. Association for Computational Linguistics. doi: 10.18653/v1/2024.findings-acl.19. URL  
 540 <https://aclanthology.org/2024.findings-acl.19>.
- 541 Clara Meister, Ryan Cotterell, and Tim Vieira. If beam search is the answer, what was the question? In  
 542 Bonnie Webber, Trevor Cohn, Yulan He, and Yang Liu (eds.), *Proceedings of the 2020 Conference on*  
 543 *Empirical Methods in Natural Language Processing (EMNLP)*, pp. 2173–2185, Online, November 2020.  
 544 Association for Computational Linguistics. doi: 10.18653/v1/2020.emnlp-main.170. URL <https://aclanthology.org/2020.emnlp-main.170>.
- 545 Jooyoung Moon, Jihyo Kim, Younghak Shin, and Sangheum Hwang. Confidence-aware learning for deep  
 546 neural networks. In *International Conference on Machine Learning*, 2020.
- 547 openai. Learning to reason with llm, 2024. URL <https://openai.com/index/learning-to-reason-with-l1ms/>.
- 548 Long Ouyang, Jeffrey Wu, Xu Jiang, Diogo Almeida, Carroll Wainwright, Pamela Mishkin, Chong  
 549 Zhang, Sandhini Agarwal, Katarina Slama, Alex Ray, John Schulman, Jacob Hilton, Fraser Kel-  
 550 ton, Luke Miller, Maddie Simens, Amanda Askell, Peter Welinder, Paul F Christiano, Jan Leike,  
 551 and Ryan Lowe. Training language models to follow instructions with human feedback. In  
 552 S. Koyejo, S. Mohamed, A. Agarwal, D. Belgrave, K. Cho, and A. Oh (eds.), *Advances in*  
 553 *Neural Information Processing Systems*, volume 35, pp. 27730–27744. Curran Associates, Inc.,  
 554 2022. URL [https://proceedings.neurips.cc/paper\\_files/paper/2022/file/b1efde53be364a73914f58805a001731-Paper-Conference.pdf](https://proceedings.neurips.cc/paper_files/paper/2022/file/b1efde53be364a73914f58805a001731-Paper-Conference.pdf).

- 564 Gabriel Poesia, Alex Polozov, Vu Le, Ashish Tiwari, Gustavo Soares, Christopher Meek, and Sumit Gul-  
 565 wanii. Synchromesh: Reliable code generation from pre-trained language models. In *International*  
 566 *Conference on Learning Representations*, 2022. URL <https://openreview.net/forum?id=KmtVD97J43e>.
- 567
- 568 Ansh Radhakrishnan, Karina Nguyen, Anna Chen, Carol Chen, Carson E. Denison, Danny Hernandez, Esin  
 569 Durmus, Evan Hubinger, John Kernion, Kamil.e Lukovsiut.e, Newton Cheng, Nicholas Joseph, Nicholas  
 570 Schiefer, Oliver Rausch, Sam McCandlish, Sheer El Showk, Tamera Lanham, Tim Maxwell, Venkat  
 571 Chandrasekaran, Zac Hatfield-Dodds, Jared Kaplan, Janina Brauner, Sam Bowman, and Ethan Perez.  
 572 Question decomposition improves the faithfulness of model-generated reasoning. *ArXiv*, abs/2307.11768,  
 573 2023. URL <https://api.semanticscholar.org/CorpusID:259980634>.
- 574
- 575 Rafael Rafailov, Archit Sharma, Eric Mitchell, Christopher D Manning, Stefano Ermon, and Chelsea  
 576 Finn. Direct preference optimization: Your language model is secretly a reward model. In A. Oh, T. Naumann, A. Globerson, K. Saenko, M. Hardt, and S. Levine (eds.), *Advances in*  
 577 *Neural Information Processing Systems*, volume 36, pp. 53728–53741. Curran Associates, Inc.,  
 578 2023. URL [https://proceedings.neurips.cc/paper\\_files/paper/2023/file/a85b405ed65c6477a4fe8302b5e06ce7-Paper-Conference.pdf](https://proceedings.neurips.cc/paper_files/paper/2023/file/a85b405ed65c6477a4fe8302b5e06ce7-Paper-Conference.pdf).
- 579
- 580
- 581 Noah Siegel, Oana-Maria Camburu, Nicolas Manfred Otto Heess, and Maria Perez-Ortiz. The probabilities  
 582 also matter: A more faithful metric for faithfulness of free-text explanations in large language mod-  
 583 els. *ArXiv*, abs/2404.03189, 2024. URL <https://api.semanticscholar.org/CorpusID:268889439>.
- 584
- 585 Miles Turpin, Julian Michael, Ethan Perez, and Samuel Bowman. Language models don't al-  
 586 ways say what they think: Unfaithful explanations in chain-of-thought prompting. In A. Oh,  
 587 T. Naumann, A. Globerson, K. Saenko, M. Hardt, and S. Levine (eds.), *Advances in Neu-*  
 588 *ral Information Processing Systems*, volume 36, pp. 74952–74965. Curran Associates, Inc.,  
 589 2023. URL [https://proceedings.neurips.cc/paper\\_files/paper/2023/file/ed3fea9033a80fea1376299fa7863f4a-Paper-Conference.pdf](https://proceedings.neurips.cc/paper_files/paper/2023/file/ed3fea9033a80fea1376299fa7863f4a-Paper-Conference.pdf).
- 590
- 591 Jun Wang, Meng Fang, Ziyu Wan, Muning Wen, Jiachen Zhu, Anjie Liu, Ziqin Gong, Yan Song, Lei Chen,  
 592 Lionel M. Ni, Linyi Yang, Ying Wen, and Weinan Zhang. Openr: An open source framework for ad-  
 593 vanced reasoning with large language models. 2024. URL <https://api.semanticscholar.org/CorpusID:273345614>.
- 594
- 595 Adina Williams, Nikita Nangia, and Samuel Bowman. A broad-coverage challenge corpus for sentence  
 596 understanding through inference. In Marilyn Walker, Heng Ji, and Amanda Stent (eds.), *Proceed-  
 597 ings of the 2018 Conference of the North American Chapter of the Association for Computational  
 598 Linguistics: Human Language Technologies, Volume 1 (Long Papers)*, pp. 1112–1122, New Orleans,  
 599 Louisiana, June 2018. Association for Computational Linguistics. doi: 10.18653/v1/N18-1101. URL  
 600 <https://aclanthology.org/N18-1101>.
- 601
- 602 Yuxi Xie, Anirudh Goyal, Wenyue Zheng, Min-Yen Kan, Timothy P. Lillicrap, Kenji Kawaguchi, and  
 603 Michael Shieh. Monte carlo tree search boosts reasoning via iterative preference learning. *ArXiv*,  
 604 abs/2405.00451, 2024. URL <https://api.semanticscholar.org/CorpusID:269484186>.
- 605
- 606 Hanqi Yan, Qinglin Zhu, Xinyu Wang, Lin Gui, and Yulan He. Mirror: Multiple-perspective self-reflection  
 607 method for knowledge-rich reasoning. In Lun-Wei Ku, Andre Martins, and Vivek Srikumar (eds.), *Pro-  
 608 ceedings of the 62nd Annual Meeting of the Association for Computational Linguistics (Volume 1: Long  
 609 Papers)*, pp. 7086–7103, Bangkok, Thailand, August 2024. Association for Computational Linguistics.  
 610 doi: 10.18653/v1/2024.acl-long.382. URL <https://aclanthology.org/2024.acl-long.382>.

- 611 Shunyu Yao, Jeffrey Zhao, Dian Yu, Nan Du, Izhak Shafran, Karthik R Narasimhan, and Yuan Cao. React:  
612 Synergizing reasoning and acting in language models. In *The Eleventh International Conference on*  
613 *Learning Representations*, 2023. URL [https://openreview.net/forum?id=WE\\_vluYUL-X](https://openreview.net/forum?id=WE_vluYUL-X).
- 614 Lifan Yuan, Yangyi Chen, Ganqu Cui, Hongcheng Gao, FangYuan Zou, Xingyi Cheng, Heng Ji, Zhiyuan  
615 Liu, and Maosong Sun. Revisiting out-of-distribution robustness in nlp: Benchmarks, analysis, and llms  
616 evaluations. In A. Oh, T. Naumann, A. Globerson, K. Saenko, M. Hardt, and S. Levine (eds.), *Advances in Neural Information Processing Systems*, volume 36, pp. 58478–58507. Curran Associates, Inc.,  
617 2023. URL [https://proceedings.neurips.cc/paper\\_files/paper/2023/file/b6b5f50a2001ad1cbcca96e693c4ab4-Paper-Datasets\\_and\\_Benchmarks.pdf](https://proceedings.neurips.cc/paper_files/paper/2023/file/b6b5f50a2001ad1cbcca96e693c4ab4-Paper-Datasets_and_Benchmarks.pdf).
- 618 Di Zhang, Jianbo Wu, Jingdi Lei, Tong Che, Jiatong Li, Tong Xie, Xiaoshui Huang, Shufei Zhang, Marco  
619 Pavone, Yuqiang Li, Wanli Ouyang, and Dongzhan Zhou. Llama-berry: Pairwise optimization for o1-  
620 like olympiad-level mathematical reasoning. *ArXiv*, abs/2410.02884, 2024a. URL <https://api.semanticscholar.org/CorpusID:273162606>.
- 621 Shaolei Zhang, Tian Yu, and Yang Feng. TruthX: Alleviating hallucinations by editing large language  
622 models in truthful space. In Lun-Wei Ku, Andre Martins, and Vivek Srikumar (eds.), *Proceedings of*  
623 *the 62nd Annual Meeting of the Association for Computational Linguistics (Volume 1: Long Papers)*,  
624 pp. 8908–8949, Bangkok, Thailand, August 2024b. Association for Computational Linguistics. doi: 10.  
625 18653/v1/2024.acl-long.483. URL <https://aclanthology.org/2024.acl-long.483>.
- 626 Xuandong Zhao, Xianjun Yang, Tianyu Pang, Chao Du, Lei Li, Yu-Xiang Wang, and William Yang Wang.  
627 Weak-to-strong jailbreaking on large language models. *arXiv preprint arXiv:2401.17256*, 2024.

---

658 APPENDIX  
659  
660  
661

662 A EXPERIMENT SETUP  
663

664 We utilize a comprehensive experiment approach with seven datasets across three distinct reasoning tasks.  
665 The backbone models adopted for experiments, dataset details, counterfactual generation algorithms and  
666 hyper-parameters setting are outlined below.

667 **Backbone model choice.** Our experiments select two commonly used backbone model choices, Llama3-  
668 8B Instruct model<sup>6</sup> and Mistral 7B Instruct model<sup>7</sup> models. Both models are downloaded from the Hugging-  
669 Face Models’ space, and we used the Huggingface Transformer<sup>8</sup> to implement the models.

670  
671 **Hyper-parameters for inference.** For efficient model inference, we applied 8-bit quantization on both the  
672 backbone and global reward models for *Our+Expert* and *Our(full)* experiments. The local reward models are  
673 loaded without any quantization. We set a maximum allowance of 10 different particles during decoding,  
674 which means it will keep a maximum of 10 different paths during the search through different weighted  
675 decoding paths. The beam factor for expanding searching at each particle is set as 3. To optimize the  
676 computational resources for generation, we applied different maximum token length sizes for each task,  
677 which we will introduce under each task. Also, our local rewards will be disabled once the answer token is  
678 generated to remove the token space constraint. We use a batch size of 64 to inference our framework on a  
679 single NVIDIA A100 40G graphic card. The random seed has been set as 42 for all the components.

680  
681 **Predicted label evaluation details.** Apart from the faithfulness evaluation details presented in Section 4,  
682 the evaluation for the predicted label is extracted and compared with the ground-truth label to calculate the  
683 accuracy score. Following each prompt template, we designed a regular expression to extract the score/labels  
684 from the generated sequence. If the model fails to follow the prompt to generate a valid label token, then it  
685 counts as a wrongly predicted instance. In short, only correctly predicted instances that follow the prompt  
686 required output pattern count towards the accuracy score.

687 A.1 STUDENT ANSWER ASSESSMENT SETUP  
688

689 We employed the ASAP<sup>9</sup> dataset to evaluate our methods’ effectiveness. Following the rationale generation  
690 paradigm established by Li et al. (2023), we adopted the same rationale generation prompt used in their  
691 study, focusing on four subsets of science and biology questions. For each dataset, we randomly selected 100  
692 instances from the test split. All the local and global reward models are trained on a training set without data  
693 contamination. Our analysis shows that previous zero-shot students’ answer assessment rationale generation  
694 method typically generates rationales with an average sequence length of less than a hundred. Therefore, we  
695 set the maximum token length for this task as 100.

696  
697 **Prompt template.** We use the following prompt template applied to all our test instances. The question,  
698 key\_elements, marking\_rubric, and student\_answer correspond to question-dependent information from the  
699 dataset:

700  
701 <sup>6</sup><https://huggingface.co/meta-llama/Llama-3.1-8B-Instruct>  
702

703 <sup>7</sup><https://huggingface.co/mistralai/Mistral-7B-Instruct-v0.3>  
704

705 <sup>8</sup><https://huggingface.co/docs/transformers/index>  
706

707 <sup>9</sup><https://kaggle.com/competitions/asap-sas>  
708

705 [Question]:  $\{question\}$

706 [Key Elements]:  $\{key\_elements\}$

707 [Marking Rubric]:  $\{marking\_rubric\}$

708 [Student Answer]:  $\{student\_answer\}$

709 Please assess this student response and provide rationale, in the format of “x point/s; rationale”:

710  
 711 **Local and global reward model setup.** We utilize a text classifier fine-tuned on the ASAP datasets,  
 712 built on DeBERTa-v3-large model (He et al., 2023) as the local reward model. We adopted two global  
 713 model choices: **Choice 1**: An open-source explainable student answer scoring LLM developed by Li et al.  
 714 (2024a). The model is fine-tuned using synthetically generated student answer data with 4-bit quantization  
 715 with LoRA. **Choice 2**: A mistral 7B model fine-tuned on science question and answer: Weyaxi/Einstein-v2-  
 716 7B. The model is fine-tuned with a science question-and-answer dataset based on the Mistral 7B model.  
 717

718  
 719 **Sentence-level perturbation for student answer assessment dataset.** Our evaluation strategy involved  
 720 systematically modifying key parts from student answers  $x_i$  in the input data by comparing each key answer  
 721 element  $k_i$  from all key elements  $K$ . Then, observe the resultant variations in the generated rationales. By  
 722 doing so, we could ascertain whether the rationales remained consistent and aligned with the altered inputs,  
 723 thereby providing insights into their reliability and interpretability. This approach ensures that the rationales  
 724 are contextually relevant and robust against variations in input, thereby enhancing their practical utility in  
 725 real-world applications.

---

## 726 Algorithm 2 Student Answer Perturbation Algorithm

---

727  
 728 1: **procedure** PERTURBATION( $x_i, K$ )  
 729 2:      $\mathbf{S} \leftarrow \text{Tokenize}(x_i)$   
 730 3:      $\mathbf{I} \leftarrow \text{array of zeros with length}(|\mathbf{S}|)$   
 731 4:     **for**  $j \leftarrow 1$  to  $|\mathbf{S}|$  **do**  
 732         **for**  $k \leftarrow 1$  to  $|K|$  **do**  
 733              $\mathbf{I}[j] \leftarrow \mathbf{I}[j] + \text{Sim}(\mathbf{S}[j], K[k])$   
 734         **end for**  
 735     **end for**  
 736      $i_{\max} \leftarrow \text{argmax}(\mathbf{I})$   
 737      $\mathbf{S} \leftarrow \mathbf{S} \setminus \{\mathbf{S}[i_{\max}]\}$   
 738      $\hat{\mathbf{S}} \leftarrow \text{Join}(\mathbf{S})$   
 739     **return**  $\hat{\mathbf{S}}$   
 740 13: **end procedure**

---

## 741 742 A.2 NATURAL LANGUAGE INFERENCE (NLI)

743  
 744 For NLI, we utilized two key datasets: the Stanford Natural Language Inference (*SNLI*) (Bowman et al.,  
 745 2015) and the Multi-Genre Natural Language Inference (*MNLI*) (Williams et al., 2018) datasets. These  
 746 datasets are critical for assessing the ability of our models to handle a range of inferential relationships  
 747 across various genres, thus providing a comprehensive view of model performance in understanding lan-  
 748 guage context. We randomly selected 100 instances from the official validation split for each dataset; for the  
 749 *MNLI* dataset, we used the matched validation set. We find existing explanations from the ESNLI dataset  
 750 have an average sequence length shorter than 30 tokens. Therefore, we employed the maximum token length  
 751 of 30 for the NLI task.

752     **Prompt template.** We use the following prompt template to evaluate our method on all the NLI tasks. The  
 753     premise and hypothesis placeholder corresponds to the premise and hypothesis from each row.  
 754

755     **Here is a premise:** {*premise*}  
 756     **Here is a hypothesis:** {*hypothesis*}  
 757     Please choose whether the hypothesis is entailment, neutral, or contradiction to the premise, and provide a  
 758     rationale for your choice. Output the label and rationale in the format of “Prediction: [label]; [explanation]”;  
 759     Prediction:

760     **Local and global reward model setup.** We use an open-source fine-tuned BART model (Lewis et al.,  
 761     2020) for performing classification in NLI tasks as the local reward model. Please refer to their released  
 762     repository for detailed training data usage and splits. For the global model, we utilize a LORA fine-tuned  
 763     Llama-2-7B model on the ESNLI dataset Camburu et al. (2018). The model is trained solely on the training  
 764     set of the ESNLI. To reduce computational resources, the local reward model is disabled after generating the  
 765     answer token.  
 766

767     **Hyper-parameters for inference.** For efficient model inference, we applied 8-bit quantization on both the  
 768     backbone and global reward models. The local model is loaded without quantization. We set a maximum  
 769     allowance of 10 different particles during decoding. The beam factor for searching is set as 3, with a  
 770     maximum token length of 30.

771     **Word-level perturbation for NLI tasks.** For *NLI*, we identify a keyword among adjective and verb words  
 772     by POS-tagging using *TokenizeAndTag*. The adj and adv word lists are imported from the nltk package. Once  
 773     the words are tagged, we randomly insert an irrelevant adjective word into either the premise or hypothesis  
 774     to create such perturbation using the *GenerateExample* function. The *GenerateExample* function takes the  
 775     whole token lists and the randomTarget word and position to reconstruct the perturbed sequence. Our goal  
 776     is to detect the modified word from the generated rationale to evaluate the faithfulness of our method.  
 777

---

778     **Algorithm 3** NLI Word Perturbation Generation

---

779     1: **procedure** PERTURBATION( $x_i$ , adj, adv)  
 780       2:     tokens, tags  $\leftarrow$  TokenizeAndTag( $x_i$ )  
 781       3:     targets  $\leftarrow$  IdentifyTargets(tags, adj, adv)  
 782       4:     randomTarget  $\leftarrow$  SampleTargets(targets)  
 783       5:     example  $\leftarrow$  GenerateExample(tokens, randomTarget)  
 784       6:     **return** example  
 785     7: **end procedure**

---

787     A.3 QA

789     The *TruthfulQA* dataset contains questions and answers. Each question has multiple answers, which were  
 790     adapted into a multiple-choice format. The model’s task for this dataset is to select the most truthful answer  
 791     through all the options.  
 792

793     **Prompt template.** We use the following prompt template to evaluate our method on the QA task. The  
 794     question is the question row from the dataset, and the choices are selections for answers from the dataset.  
 795

796     **Question:** {*question*}  
 797     **Choose the best answer from following options:** {*choices*}  
 798     Output the selection with reason in the format of Answer: “choice; reason”. Answer:

**Local and global reward model setup.** We use an open-source truth judge released by Allen AI: allenai/truthfulqa-truth-judge-llama2-7B. For the global model, we utilize a 7B LLM specialized in truthful QA, released by Zhang et al. (2024b). Please refer to the original paper for the detailed training setup and dataset split for the local and global models. To reduce computational resources, the local reward model is disabled after generating the answer token.

**Hyper-parameters for inference.** For efficient model inference, we applied 8-bit quantization on both the backbone and global reward models. The local model is loaded without quantization. We set a maximum allowance of 10 different particles during decoding. The beam factor for searching is set as 3, with a maximum token length of 30.

**Word-level perturbation for QA task.** For *QA* task, we identify an influential word to be replaced, similar to the Algorithm 3. Instead of using an algorithm to perturb the word, in this task, we query the GPT-4 model to modify the original sentence and output both the modified word and the perturbed sentence. Evaluating the faithfulness of the task still depends on the successful rate of reflection of modified words from the rationale.

## B ADDITIONAL EXPERIMENT RESULTS

### B.1 EFFECTS OF DIFFERENT BACKBONE MODEL

**Similar experimental result trends are also observed on other backbone models.** In addition to evaluating our method on the Llama3-8B model, we extended our investigation to other backbone models, specifically examining the Mistral 7B model. The results, summarized in Table 8, demonstrate a consistent trend across different model sizes, underscoring the robustness of our method.

The performance comparison conducted on the Mistral 7B model reveals an overall slight decrease in average performance compared to the Llama3-8B results. Despite this reduction, the relative performance enhancements provided by our method remained consistent. For instance, while the baseline Backbone model scored lower across all tasks, introducing local and global expert knowledge notably improved performance, with our method achieving the highest task performance in all the cases.

Moreover, we also evaluate the faithfulness of the rationale for *Student Answer Assessment* in Table 9 and *NLI* and *TruthfulQA* in Table 10. Similar to our observation with Llama3-8B as the backbone model, the faithfulness evaluation results highlight that our method is able to generate a more faithful rationale that could reflect the change in the input compared with the backbone model.

These findings indicate that while the inherent capabilities of the backbone models influence absolute performance metrics, the efficacy of our approach in enhancing model output by integrating classifiers and expert insights transcends the specific model used. The trend observed with the Mistral-7B, similar to that with the LLama-3-8B, validates our method’s general applicability and effectiveness across different neural architectures, highlighting its potential for broad adoption in diverse NLP tasks.

| Datasets                         | Backbone | Ours       |
|----------------------------------|----------|------------|
| <i>Student Answer Assessment</i> |          |            |
| ASAP-Q1                          | 31%      | <b>80%</b> |
| ASAP-Q2                          | 38%      | <b>69%</b> |
| ASAP-Q3                          | 35%      | <b>84%</b> |
| ASAP-Q4                          | 45%      | <b>80%</b> |
| <i>NLI</i>                       |          |            |
| SNLI                             | 47%      | <b>79%</b> |
| MNLI                             | 41%      | <b>78%</b> |
| <i>QA</i>                        |          |            |
| TruthfulQA                       | 43%      | <b>72%</b> |

Table 8: Mistral 7B model overall performance compared across each method. The best performance over text generation models is highlighted in **bold**.

846  
847  
848  
849  
850  
851  
852  
853  
854  
855  
856  
857  
858  
859  
860  
861  
862  
863  
864  
865  
866  
867  
868  
869  
870  
871  
872  
873  
874  
875  
876  
877  
878  
879  
880  
881  
882  
883  
884  
885  
886  
887  
888  
889  
890  
891  
892

| Method  | ASAP-Q1      |              |              | ASAP-Q2      |              |              | ASAP-Q3      |              |              | ASAP-Q4 |              |              |
|---------|--------------|--------------|--------------|--------------|--------------|--------------|--------------|--------------|--------------|---------|--------------|--------------|
|         | R-1          | R-2          | R-L          | R-1          | R-2          | R-L          | R-1          | R-2          | R-L          | R-1     | R-2          | R-L          |
| Mistral | 0.005        | 0.004        | 0.005        | 0.024        | 0.006        | 0.023        | 0.026        | 0.015        | 0.028        | 0.012   | 0.003        | 0.005        |
| Ours    | <b>0.046</b> | <b>0.033</b> | <b>0.042</b> | <b>0.080</b> | <b>0.078</b> | <b>0.080</b> | <b>0.032</b> | <b>0.019</b> | <b>0.034</b> | 0.010   | <b>0.012</b> | <b>0.008</b> |

Table 9: The sentence-level semantic variations measured in ROUGE scores.

| Dataset    | Mistral | Ours       |
|------------|---------|------------|
| SNLI       | 14%     | <b>15%</b> |
| MNLI       | 7%      | <b>16%</b> |
| TruthfulQA | 17%     | <b>20%</b> |

Table 10: Faithfulness on *NLI* and *TruthfulQA* tasks on word inclusive. Ours greatly enhances the faithfulness on both datasets.

## B.2 INVESTIGATE THE LEXICAL SIMILARITY

To explore the source of faithfulness enhancement, we calculate the semantics overlap between the given context and generated rationale. This is motivated by the hypothesis that a more faithful model will generate a rationale more coherent with the given question context rather than too general and nonsense words or hallucinations. Therefore, we calculate the BLEU between the generated rationale and the given prompt, including the question, student answer and instruction. Results are shown in Table 11.

| Method   | 1-gram       | 2-gram       | 3-gram       | 4-gram       |
|----------|--------------|--------------|--------------|--------------|
| Backbone | 0.106        | 0.090        | 0.058        | 0.025        |
| Ours     | <b>0.452</b> | <b>0.333</b> | <b>0.167</b> | <b>0.058</b> |

Table 11: Semantic coherence between given assessment marking criteria and generated rationale. Higher values imply higher lexical similarity.

## C GENERALISABILITY OF OUR GENERATION FRAMEWORK

### C.1 INFINITE LABEL SPACE

Our method is extendable to scenarios with an infinite label space ( $|\mathcal{C}| = \infty$ ), even though the current evaluations are performed on tasks where the label space is constrained ( $|\mathcal{C}| = N \in \mathbb{R}$ ). For instance, in mathematical problem-solving, the answer can be any arbitrary number. In such cases, the expert model provides a prediction  $M$ , with its confidence expressed as the probability  $w_1$  assigned to  $M$ , and  $w_2$  to the second most probable prediction. The ratio  $\frac{w_1}{w_2}$  serves as an indicator of the expert’s confidence in delivering  $M$  (Moon et al., 2020). This confidence is then used as a multiplier to enhance the backbone model’s prediction for  $M$ . Finally, the backbone model’s transition distribution is renormalized to maintain a valid probability distribution.

### C.2 EXPERT MODELS ACROSS DIFFERENT TOKENISATION SPACES

| Method             | ASAP-Q1      |              |              | ASAP-Q2      |              |              | ASAP-Q3      |              |              | ASAP-Q4      |              |              |
|--------------------|--------------|--------------|--------------|--------------|--------------|--------------|--------------|--------------|--------------|--------------|--------------|--------------|
|                    | R-1          | R-2          | R-L          |
| Llama3             | 0.037        | 0.043        | 0.034        | 0.052        | <b>0.050</b> | 0.052        | 0.042        | 0.031        | 0.043        | 0.006        | 0.018        | 0.001        |
| Ours (w/ Expert 2) | <b>0.124</b> | <b>0.142</b> | <b>0.126</b> | <b>0.065</b> | 0.025        | <b>0.063</b> | <b>0.090</b> | <b>0.097</b> | <b>0.092</b> | <b>0.104</b> | <b>0.116</b> | <b>0.107</b> |

Table 12: The sentence-level semantic variations measured in ROUGE scores with the global expert choice 2 from the Appendix A on Student Answer Assessment.

**Different expert model for student answer assessment** As highlighted in Appendix A, the second expert model employs a distinct tokenization strategy, and the model is trained and tailored specifically for scientific

| 893 | <b>Method</b>          | <b>Time Cost</b> |
|-----|------------------------|------------------|
| 894 | Backbone (Beam Search) | 88 mins          |
| 895 | :+ Local               | 100 mins         |
| 896 | :+ Global              | 103 mins         |
| 897 | Ours (full)            | 116 mins         |

Table 14: Computation cost for different methods on *Student Answer Assessment* Q4.

questions and answers. To further validate our approach, a series of experiments were conducted, as detailed in Table 13, using the *Student Answer Assessment* datasets. These experiments demonstrate the compatibility of our method with domain-specific expert models. Despite a modest reduction in performance compared to the highly specialized domain-related expert model, our method consistently outperformed the Llama 3 Backbone across all datasets. Further, as presented in Table 12, we assessed the faithfulness of the rationale generated under the guidance of the second expert model. Our findings indicate that our method maintained a high level of faithfulness to the perturbations, notwithstanding the different tokenisation approaches, underscoring its robustness and adaptability in handling domain-specific challenges.

**Dealing with rewards from different tokenisation models** In our approach, we address the challenge of integrating rewards derived from various tokenization models used by expert systems. Specifically, after the generation of each token, it is converted into token IDs according to the expert model’s tokenization scheme. Subsequently, rewards are calculated based on samples drawn from the expert model. This method ensures that the generated tokens are consistently evaluated in the context of the expert’s linguistic framework, and therefore generating meaningful predicted rewards.

### C.3 COMPUTATION COST ANALYSIS

Although global and local constraints introduced new computations during the text generation processes, we didn’t observe a huge computational cost increment in our method. As shown in Figure 14, we calculated the inference time on the Student Answer Assessment question #4 to compare the time used between methods on the same GPU. We use a beam size of 3 and a maximum of 100 tokens in generation settings. Compared with the backbone model, our method only increased by 32% on inference time. Compared to other sequential Monte Carlo method, such as *PPO-MCTS* (Liu et al., 2024b), which has a  $2S$  times overhead compared to standard decoding from PPO models ( $S$  is the number of simulations), our inference-time decoding maintains both the performance and greatly improve the computation efficiency.

| Datasets                         | Backbone | Ours       |
|----------------------------------|----------|------------|
| <i>Student Answer Assessment</i> |          |            |
| ASAP-Q1                          | 28%      | <b>59%</b> |
| ASAP-Q2                          | 28%      | <b>55%</b> |
| ASAP-Q3                          | 45%      | <b>67%</b> |
| ASAP-Q4                          | 38%      | <b>56%</b> |

Table 13: Llama-3-8B performance on *Student Answer Assessment* with different global expert choices. The best performance over text generation models is highlighted in **bold**.

### D PROOF OF PRUNED MONTE CARLO SEARCH

**Definition.** We first define the notations:  $\mathcal{A}, \mathcal{B}, \mathcal{C}$  are three searched trajectories, among which one trajectory will be pruned.  $N_A, N_B, N_C$  are the number of simulations conducted on the corresponding trajectories,  $W_A, W_B, W_C$  are the total wins for the trajectories.

The estimated value of each branch, i.e., **the probability of being sampled** is defined as:

$$V_A = \frac{W_A}{N_A}, \quad V_B = \frac{W_B}{N_B}$$

940 Without loss of generalisability, we assume the initial condition and branch  $C$  be identified and pruned:  
 941

$$942 \quad V_A > V_B \implies \frac{W_A}{N_A} > \frac{W_B}{N_B}$$

943  
 944 Our proof goal is to show after pruning  $\mathcal{C}$ , the probability of sampling  $\mathcal{B}$  can be larger than  $\mathcal{A}$ .  
 945

946 Proof. After pruning  $\mathcal{C}$ , the remaining resources (i.e., simulations) are redistributed to branches  $A$  and  $B$ .  
 947 We define  $R_A$  and  $R_B$  are the additional simulations allocated to  $\mathcal{A}$  and  $\mathcal{B}$ .  
 948

949 After pruning, the new number of simulations for branches  $A$  and  $B$  are:  
 950

$$951 \quad N'_A = N_A + R_A, \quad N'_B = N_B + R_B$$

952 After pruning: we define  $W'_A$ ,  $W'_B$  as new total wins after additional simulations. Therefore, the new values  
 953 for  $\mathcal{A}$  and  $\mathcal{B}$  are as follows:  
 954

$$955 \quad V'_A = \frac{W'_A}{N_A + R_A} \quad (\text{new estimated value of A})$$

$$956 \quad V'_B = \frac{W'_B}{N_B + R_B} \quad (\text{new estimated value of B})$$

957 To establish that  $V'_B > V'_A$ , we require:  
 958

$$959 \quad \frac{W'_B}{N_B + R_B} > \frac{W'_A}{N_A + R_A}$$

960 Cross-multiplying gives:  
 961

$$962 \quad W'_B \cdot (N_A + R_A) > W'_A \cdot (N_B + R_B)$$

963 Given that  $W'_B > W_B$  and  $W'_A < W_A$ , it is possible for the following to hold true. For example, in  
 964 our NLI dataset, the undesirable labels are '*contradictory*', so we remove the trajectory  $\mathcal{C}$  consisting of  
 965 '*contradictory*'. For the remaining trajectories,  $\mathcal{A}$  and  $\mathcal{B}$  are related to '*contradictory*' and '*Neutral*' (not  
 966 exact label, but similar attitude), respectively. With the removal of '*contradictory*', the new sentence could  
 967 turn to *neutral* attitude, so the probability of selecting all '*Neutral*'-related trajectories could be largely  
 968 increased and probability of selecting all '*Neutral*'-related trajectories could be largely penalised.  
 969

970 In this case, even we increase  $W'_B$  by increasing the  $N_B$ , the substantial enhancement of  $W'_B$  still could lead  
 971 to a larger  $V'_B$ .  
 972

973 Thus, we can conclude: After pruning branch  $C$ , the additional simulations allocated to branch  $B$  can  
 974 increase its estimated value due to improved exploration, leading to:  
 975

$$976 \quad V'_B > V'_A$$

977  $\square$   
 978

979  
 980  
 981  
 982  
 983  
 984  
 985  
 986